



3-1-2003

Synthesis of Highly Porous Yttria-Stabilized Zirconia by Tape-Casting Methods

Marta Boaro
University of Pennsylvania

John M. Vohs
University of Pennsylvania, vohs@seas.upenn.edu

Raymond J. Gorte
University of Pennsylvania, gorte@seas.upenn.edu

Follow this and additional works at: https://repository.upenn.edu/cbe_papers

 Part of the [Ceramic Materials Commons](#)

Recommended Citation

Boaro, M., Vohs, J. M., & Gorte, R. J. (2003). Synthesis of Highly Porous Yttria-Stabilized Zirconia by Tape-Casting Methods. Retrieved from https://repository.upenn.edu/cbe_papers/12

Copyright The American Ceramic Society. Reprinted from *Journal of the American Ceramic Society*, Volume 86, Issue 3, March 2003, pages 395-400.

Publisher URL: <http://www.ceramicjournal.org/issues/v86n3/pdf/6739.pdf>

This paper is posted at ScholarlyCommons. https://repository.upenn.edu/cbe_papers/12
For more information, please contact repository@pobox.upenn.edu.

Synthesis of Highly Porous Yttria-Stabilized Zirconia by Tape-Casting Methods

Abstract

Porous ceramics of Y_2O_3 -stabilized ZrO_2 (YSZ) were prepared by tape-casting methods using both pyrolyzable pore formers and NiO followed by acid leaching. The porosity of YSZ wafers increased in a regular manner with the mass of graphite or polymethyl methacrylate (PMMA) to between 60% and 75% porosity. SEM indicated that the shape of the pores in the final ceramic was related to the shape of the pore formers, so that the pore size and microstructure of YSZ wafers could be controlled by the choice of pore former. Dilatometry measurements showed that measurable shrinkage started at 1300 K, and a total shrinkage of 26% was observed, independent of the amount or type of pore former used. Temperature-programmed oxidation (TPO) measurements on the green tapes demonstrated that the binders and dispersants were combusted between 550 and 750 K, that PMMA decomposed to methyl methacrylate between 500 and 700 K, and that graphite combusted above 900 K. The porosity of YSZ ceramics prepared by acid leaching of nickel from NiO-YSZ, with 50 wt% NiO, was studied as a function of NiO and YSZ particle size. Significant changes in pore dimension were found when NiO particle size was changed.

Disciplines

Ceramic Materials

Comments

Copyright The American Ceramic Society. Reprinted from *Journal of the American Ceramic Society*, Volume 86, Issue 3, March 2003, pages 395-400.

Publisher URL: <http://www.ceramicjournal.org/issues/v86n3/pdf/6739.pdf>

Synthesis of Highly Porous Yttria-Stabilized Zirconia by Tape-Casting Methods

Martha Boaro, John M. Vohs, and Raymond J. Gorte*

Department of Chemical and Biomolecular Engineering, University of Pennsylvania, Philadelphia, Pennsylvania 19104

Porous ceramics of Y_2O_3 -stabilized ZrO_2 (YSZ) were prepared by tape-casting methods using both pyrolyzable pore formers and NiO followed by acid leaching. The porosity of YSZ wafers increased in a regular manner with the mass of graphite or polymethyl methacrylate (PMMA) to between 60% and 75% porosity. SEM indicated that the shape of the pores in the final ceramic was related to the shape of the pore formers, so that the pore size and microstructure of YSZ wafers could be controlled by the choice of pore former. Dilatometry measurements showed that measurable shrinkage started at 1300 K, and a total shrinkage of 26% was observed, independent of the amount or type of pore former used. Temperature-programmed oxidation (TPO) measurements on the green tapes demonstrated that the binders and dispersants were combusted between 550 and 750 K, that PMMA decomposed to methyl methacrylate between 500 and 700 K, and that graphite combusted above 900 K. The porosity of YSZ ceramics prepared by acid leaching of nickel from NiO-YSZ, with 50 wt% NiO, was studied as a function of NiO and YSZ particle size. Significant changes in pore dimension were found when NiO particle size was changed.

I. Introduction

POROUS ceramics have a number of important applications in devices that include filters, gas burners, bioceramics, fuel-cell electrodes, and membrane reactors.¹ While there are a number of ways to synthesize porous ceramics,^{2–9} tape casting with pore formers appears to be one of the simplest and most flexible methods, and highly porous ceramics can be achieved in this way, even after high-temperature calcination.^{9,10} Tape casting can also be easily adapted to prepare multiple layers. For example, in some applications, it is desirable to attach a porous layer to a dense ceramic layer.^{11,12} By casting or laminating two layers in the green tape, porous and dense layers can be formed in a single step on calcination.

In our own work developing copper-based ceramic–metallic (cermet) composites for anodes in solid oxide fuel cells (SOFCs),^{10,13–17} the synthesis of a porous Y_2O_3 -stabilized ZrO_2 (YSZ) matrix is the first step in the fabrication of the cermet. Because the melting temperatures of Cu_2O and CuO are below those necessary for YSZ sintering, we have prepared Cu-YSZ cermets by impregnating soluble salts of copper into porous YSZ structures after the YSZ has been sintered.^{16,17} Because the cermet anode should be 30 vol% metal to ensure electronic conductivity and should still remain highly porous to allow diffusion of fuel to the electrolyte interface,¹⁸ very high initial porosity is desirable for

the YSZ before addition of CuO_x . We have focused on preparing porous YSZ by tape-casting methods, with both pyrolyzable and nonpyrolyzable pore formers.^{10,19} Carbon-based pyrolyzable pore formers are removed by combustion during high-temperature calcination. Nonpyrolyzable oxide pore formers remain in the YSZ following calcination and are removed by additional processing in a separate step.¹⁹

It is well-known that SOFC performance is affected by the structure of the anode.^{20–24} Therefore, it is very important to be able to control the overall porosity and structure of the pores in the porous YSZ matrix that is used to make the anode. In this paper, we report the results of our investigations in the fabrication of porous YSZ using both pyrolyzable and nonpyrolyzable pore formers. It is demonstrated that desirable pore structures can be obtained through the use of selected pore formers and that the size of the pores can be “fine-tuned” by changing the particle sizes of oxides in the green tape. Finally, some insights into the mechanisms of forming pores through the use of pore formers are reported.

II. Experimental Procedure

The properties of the YSZ and NiO used in this study are shown in Table I. The YSZ was an 8 mol% YSZ (8% Y; TZ-8T, Tosoh Corp., Tokyo, Japan), and the NiO was obtained (Alfa Aeser, Ward Hill, MA). To increase the particle size, some powders were heated to 1823 K for 12 h. Smaller particle sizes were obtained through ball milling for 3 d in distilled water using 0.5 mm YSZ balls. The mean particle sizes and particle size distributions were determined by a particle analyzer (Model Horiba LA920, Delta Analytical, Inc.). The particle size distributions were expressed as the ratio of the standard deviation in the particle size to the mean particle size. The carbon-based pore formers were graphite (325 mesh, conductivity grade; GE, Alfa Aeser), polyethylene (low density, <300 μm ; PE, Alfa Aeser), and polymethyl methacrylate (MW of 540 000; PMMA, Scientific Polymer Products, Inc., Ontario, NY).

The tapes were prepared using a dispersant (Duramax 3005, Rohm & Haas, Philadelphia, PA) and binders (HA12 and B1000, Rohm & Haas). The relative amounts of each component are shown in Table II for a tape with 36 wt% pore former, with the concentration of pore former given as the ratio of weights for pore former to pore former and oxide. In all cases, the relative amounts of each component in the tapes were the same except for the amount of pore former added. Slurries were prepared by mixing YSZ powders with the pore former in distilled water and dispersant. After stirring the mixtures for 1 d, the binders were added to the slurry, followed by additional stirring for 9–12 h. The slurries were cast manually onto a Mylar sheet to give a tape that resulted in a thickness of 600 μm for the fired ceramic. After drying, the green tapes were cut into round or rectangular pieces, heated to 1823 K at 2 K/min, held at this temperature for 4 h, and finally cooled to room temperature at 2 K/min.

R. A. Cutler—contributing editor

Manuscript No. 186739. Received August 19, 2002; approved November 25, 2002. Supported by DARPA, under the Palm Power Program.

*Member, American Ceramic Society.

Table I. Particle Size of Oxide Samples Used in This Study

Sample	Average particle size (μm)	CV [‡]
YSZ(A), as-purchased	0.58 [†]	113.8 [†]
YSZ(C), calcined	49	75.3
YSZ(B), ball-milled	0.26	117
NiO(A), as-purchased	4.3 [†]	
NiO(C), calcined	17	50.6
NiO(B), ball-milled	1.2	47.4

[†]Information supplied by vendor. [‡]CV is defined as the ratio of standard deviation in particle size to average particle size.

The stirring times for the slurries were chosen to ensure a smooth homogeneous mixture for tape casting. Additional evidence that both the YSZ and pore former powders were well-dispersed came from the uniform appearance of the final porous ceramics that were produced from the tapes. Even though the surface concentrations for the dispersant must have changed with oxide particle size and pore former loading, well-dispersed mixtures were obtained in all cases, except with high loadings of polyethylene. The high flexibility of acrylic emulsions for tape casting has been recognized in the literature.^{11,12}

To produce NiO-YSZ composites, we used the same procedure given elsewhere.¹⁹ For the present experiments, the weight ratio of NiO and YSZ was always 1:1, and the green tapes were prepared in a manner identical to that described above and in Table II, with a NiO-YSZ mixture replacing the YSZ. In all cases, 20 wt% graphite was added to the mixture, and a good slurry dispersion was observed for all particle sizes. After calcining the green tapes to 1823 K in air, each sample was reduced in H₂ at 973 K for 10 h to convert the NiO into nickel. The nickel was removed from the Ni-YSZ cermets by acid leaching, taking advantage of the fact that ZrO₂ is insoluble in acid solutions. Approximately 0.5 g of Ni-YSZ wafers was placed in 50 mL of 2.2M HNO₃ at 353 K for 2 h.

The removal of the pore formers and binders was studied using temperature-programmed oxidation (TPO). In these experiments, ~0.4 g of tape was placed in a tube furnace and heated at 10 K/min to 1173 K. At the entrance to the furnace, the gas flow rate was 30 mL/min and consisted of 20 vol% O₂ in helium. The gas composition at the exit was monitored using a quadrupole mass spectrometer to determine the O₂ consumption and products formed.

The sintering behavior of the tapes was determined using a dilatometer (Model 2016, Orton Research Inc., Cambridge, MA) at a constant heating rate of 3 K/min. All dilatometry specimens were round pellets, ~0.2 cm thick, and 1.0 cm in diameter. SEM images of the dense and porous YSZ layers were obtained using a microscope (Model 6300/400, JEOL, Tokyo, Japan).

The porosities in this paper were measured using water immersion by calculating the porosity from the weights of the dry sample and the water-saturated sample. To ensure water saturation, the samples were immersed in boiling water and allowed to cool in water before weighing. Porosities measured by this method were reproducible within 1% and were found to be consistently 10%

Table II. Standard Composition Used in Tape Casting

Function	Materials	Amount (g)	Density (g/mL)
Oxide powder	TZ-8T	18.2	5.9
Pore former	GE	10.5 [†]	2.2
	PE		0.9
	PMMA		1.2
Solvent	Water	30	
Dispersant	Duramax 3005	1.27	1.6
Binders	HA12	3.85	1.06
	B1000	5.73	1.05

[†]Corresponds to 36 wt% of organic pore former.

lower than porosities obtained from mercury porosimetry.¹⁹ Obviously, closed pores could not be observed by either technique.

III. Results

(1) Pyrolyzable Pore Formers

As an initial indicator of the temperature at which densification of the YSZ ceramic occurred, we performed dilatometry measurements on selected samples, with the results shown in Fig. 1. The samples examined in Fig. 1 used the as-received YSZ(A) powder, and only the type and amount of pyrolyzable pore formers were changed. Because these measurements showed shrinkage in only one dimension, without a substrate to constrain shrinkage, the data should be considered a qualitative measure of sintering only. All changes observed in this study were irreversible and much larger than reversible thermal expansions, which would be ~1% for a 1000° temperature change. The data showed that shrinkage of the tapes was negligible below 1300 K, so that most densification occurred above this temperature. Furthermore, shrinkage was ~26% for all the samples tested. The presence of pore formers had no effect on the dilatometry results to a first approximation. This agreed with an earlier report from the literature, which explained the finding as resulting from a constant packing density for the ceramic powder in pore walls.⁷

We also examined the shrinkage of tapes made with ball-milled YSZ(B), precalcined YSZ(C), and 50:50 mixtures of YSZ(B) and YSZ(C). The shrinkage of tapes made with YSZ(B) was very similar to what we observed in Fig. 1. Densification occurred in the same temperature range as with the untreated YSZ, and the total shrinkage, ~26%, was essentially the same as with YSZ(A). We were unsuccessful in preparing ceramic wafers from YSZ(C). Calcination of tapes prepared with YSZ(C) resulted in only powders, even after attempts to change the relative amounts of binder and dispersant; however, we did not investigate the reasons for our inability to form ceramics from YSZ(C), whether the high-temperature treatment of this powder affected the surface chemistry of the oxide or some other property.²⁵ Finally, ceramic wafers could be produced from tapes made with 50:50 mixtures of YSZ(B) and YSZ(C), but the total shrinkage observed in dilatometry measurements was only ~10% after heating to 1823 K. Others also reported decreases in tape shrinkage when using precalcined powders.²⁶ Because the much lower shrinkage observed in this

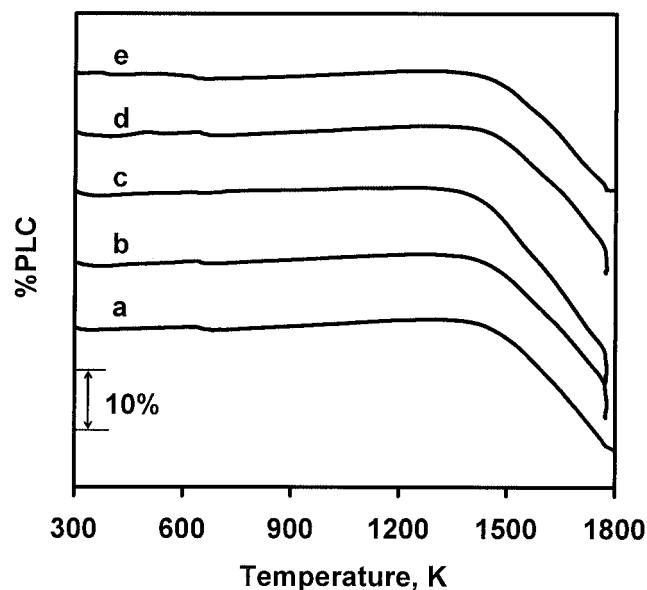


Fig. 1. Percent linear coefficient (PLC) of shrinkage ($= \Delta L/L_i$; L_i = initial length) for YSZ green tapes containing (a) no pore formers, (b) 10 wt% graphite, (c) 36 wt% graphite, (d) 10 wt% PMMA, and (e) 36 wt% PMMA.

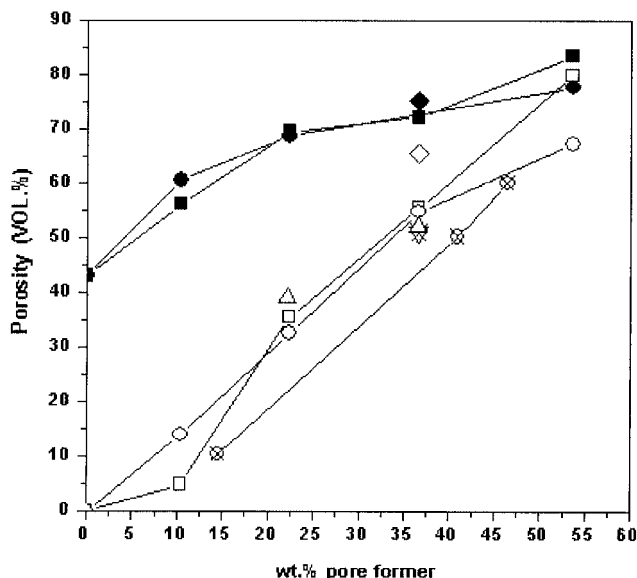


Fig. 2. Porosity after calcination at 1823 K (open symbols) and after calcination at 1523 K (black symbols) as function of weight percentage of pore formers in green tapes made the following: (○) graphite and YSZ(A); (□) PMMA, YSZ(A); (△) PMMA and YSZ(B); (◇) PMMA and a 1:1 mixture of YSZ(B) and YSZ(C); (⊗) PMMA and graphite, YSZ(A); (×) graphite and YSZ(B); △ polyethylene and YSZ(A).

mixture would make it difficult to produce ceramic bilayers with tapes produced from either pure YSZ(A) or YSZ(B), we did not pursue this further.

Figure 2 and Table III show the porosity of ceramic wafers prepared using the various pore formers and a calcination temperature of either 1523 or 1823 K. In agreement with the dilatometry results, 1523 K calcinations were insufficient to make the resulting ceramics dense, even when pore formers were not included in the green tape. For samples calcined at 1823 K, porosity was negligible in the absence of pore formers and increased almost linearly with the amount of added pore former over the range of concentrations examined. No significant differences were observed in the

Table III. Porosity of YSZ Ceramics as a Function of the Type and Amount of Pore Former Used[†]

Amount of pore former (wt%) [§]	Porosity (%) [‡]			
	PMMA	Graphite	Polyethylene	PMMA + graphite
1523 K				
0	43.1	43.1		
10.3	56.1	59.7		
22.3	69.4	61.3		
36.5	72.1	68.6		
	74.5 [¶]			
	75.2 ^{††}			
53.5	83.4	68.7		
1823K				
0	0	0	0	0
10.3	4.8	13.9		
14.53				10.4
22.3	35.5	32.6	39.1	
36.5	55.4	54.8	52.0	
	52.8 [¶]	51.1 [‡]		
	68.5 ^{††}			
40.9				50.9
46.4				60.2
53.5	79.9	67.2		

[†]Unless otherwise noted, samples were made with YSZ(A). [‡]Porosity measurements were reproducible to within ~1%. Standard deviation calculated for an average of 15 samples of the same composition is <4%. [§]Volume percentage of pore former in the green tape can be calculated from the masses and relative densities shown in Table I. [¶]Made with YSZ(B). ^{††}Made with a 1:1 mixture of YSZ(B) and YSZ(C).

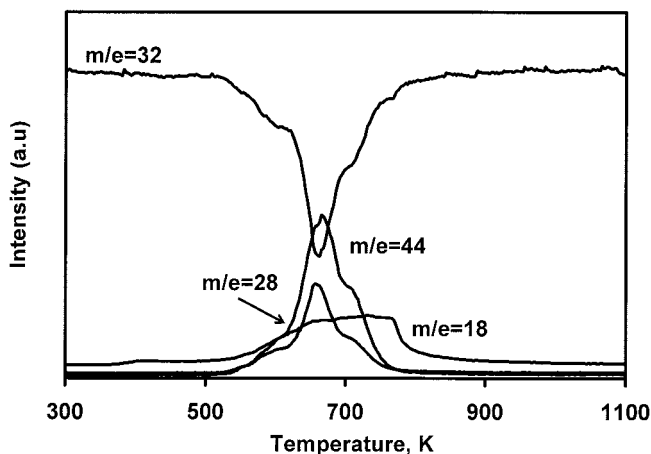


Fig. 3. TPO result for green tape without pore formers.

porosity of ceramics made from YSZ(A) or YSZ(B). While the final porosity after calcination to 1823 K did not depend strongly on which pyrolyzable pore former was used, higher porosities were obtained for PMMA than for graphite, probably due to PMMA having a lower density.

For the data in Table III, the relative amounts of binders, dispersants, and YSZ were fixed. To determine how additional binders and dispersants would affect the results, ceramic samples were made without pore formers but with a threefold increase in the amounts of binders and dispersants compared with the amounts shown in Table II. After calcination to 1823 K, the porosity of these samples was 45 vol%, a value close to that which would be obtained on a sample containing an amount of pore former equal to the additional binders and dispersants that were added. Obviously, the polymers present in the excess binders and dispersants that we used could themselves act as pore formers, showing that the amounts of added binders and dispersants must be carefully controlled.

TPO measurements were performed to determine the temperature at which the pore formers were removed and to provide insights into the mechanism by which they were removed. Figure 3 shows results for calcination of a green tape made without pore formers. Clearly, O₂ (m/e = 32) was consumed, and CO₂ (m/e = 28,44), CO (m/e = 28), and H₂O (m/e = 18) were formed between 600 and 800 K, corresponding to the removal of the dispersants and binders. Graphite was added to the green tape, and the TPO results are those shown in Fig. 4. The addition of graphite gave rise to O₂ consumption and CO and CO₂ formation at a temperature >900 K, in addition to the O₂ consumption features between 600

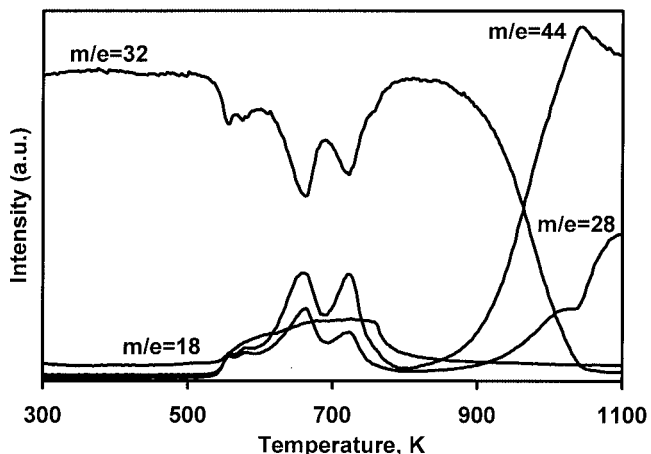


Fig. 4. TPO result for green tape with 36 wt% graphite as pore former.

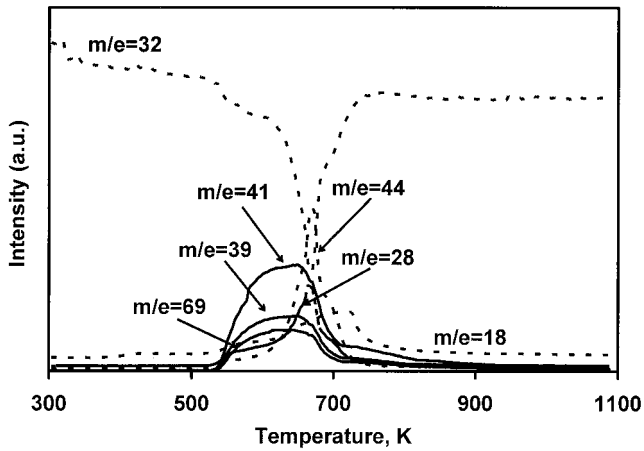


Fig. 5. TPO result for green tape with 36 wt% PMMA as pore former.

and 800 K due to the dispersants and binders. The TPO result for a tape made with PMMA (Fig. 5) showed that the PMMA decomposed to methyl methacrylate ($m/e = 41, 39, 69$).^{27,28} Because PMMA was not combusted, significantly less O_2 was consumed during calcination of the tape with PMMA compared with that observed for a tape with a similar amount of graphite. A TPO of pure PMMA also showed decomposition to methyl methacrylate, with negligible combustion, in exactly the same temperature range as shown in Fig. 5 (between 500 and 700 K).

To determine the relationship between ceramic microstructure and the type of pore former used, selected ceramic wafers were

examined by SEM. The micrographs of wafers prepared using YSZ(A) and either 36 wt% PMMA or 36 wt% graphite are shown in Fig. 6, along with micrographs of the pore-forming powders themselves. Figure 6(a) indicates that materials prepared with PMMA show large spherical cavities between 50 and 100 μm in diameter. The cavities were very similar in shape and slightly smaller than the PMMA particles (see Fig. 6(b)). Indeed, the fact that the PMMA particles were somewhat larger than the spherical cavities produced in the ceramic could be explained easily by the fact that shrinkage occurred in the ceramic at temperatures well above those at which the PMMA was removed. By contrast, the pores formed by the graphite particles were much smaller, as shown in Fig. 6(c). In agreement with mercury porosimetry data performed on similar samples prepared using the same starting materials,¹⁹ the material made with graphite had relatively uniform pores, with an average pore size of $\sim 1 \mu\text{m}$ in diameter. Figure 6(d) shows that the graphite particles were again similar in size to the pores that they formed. Not surprisingly, materials made with a mixture of PMMA and graphite pore formers had both small and large pores, as shown in Fig. 7.

Finally, materials made with the ball-milled YSZ(B) were more uniform in appearance but were otherwise identical to those made using YSZ(A). The better uniformity was likely the result of the breaking up of agglomerates in the starting YSZ powder.

(2) NiO as Pore Former

Our group has recently demonstrated that porous YSZ could be prepared by first forming a Ni-YSZ cermet, then removing the nickel by leaching in boiling HNO_3 .¹⁹ In this case, NiO acted as the pore former for YSZ. Unlike the case with pyrolyzable pore formers, NiO remained in the YSZ structure at the temperatures

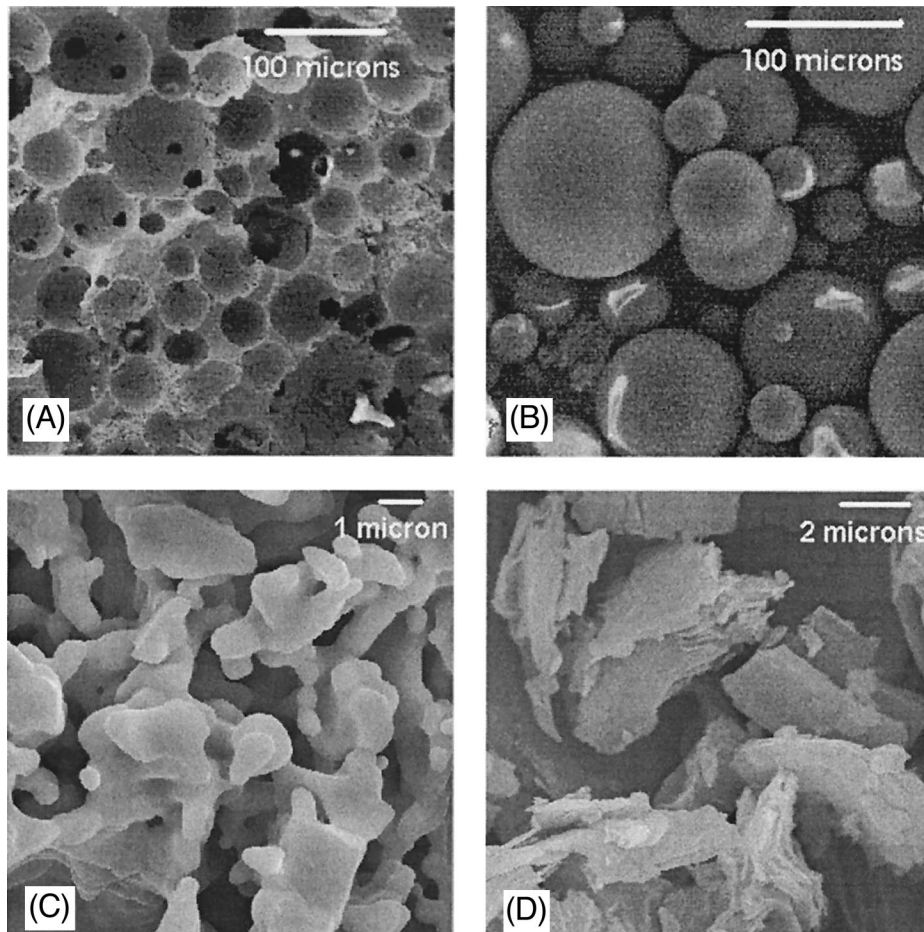


Fig. 6. SEM of (a) YSZ(A) ceramic made with 36 wt% PMMA, (b) PMMA, (c) YSZ(A) ceramic made with 36 wt% graphite, and (d) graphite.

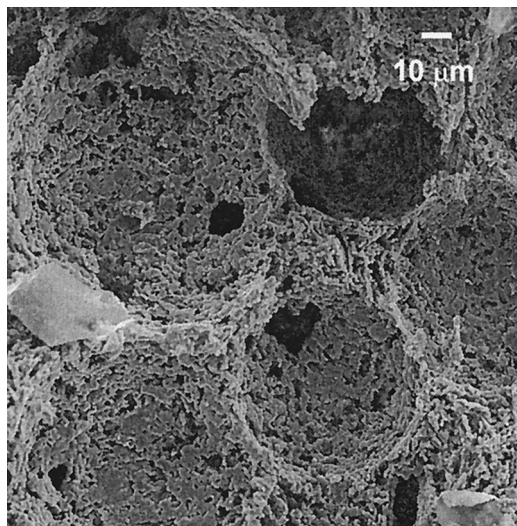


Fig. 7. SEM of YSZ(A) ceramic made from green tape containing graphite (21 wt%) and PMMA (28 wt%).

where YSZ densification occurred. Because the oxide particle sizes could be controlled, it was expected that this method could also allow control of pore size and pore size distribution. In the present study, the NiO:YSZ ratio was maintained at 1.0, and the same procedure described previously was used to make all the tapes.¹⁹

We found that the nickel could be effectively removed from all the samples prepared in this study. After reduction and acid leaching, the weight of the ceramic samples decreased by exactly 50% within experimental error (<1%). The final porosities achieved after acid leaching, shown in Table IV, depended only on which NiO powder was used to prepare the ceramic. When ball-milled NiO(B) was used, porosities were $55\% \pm 2\%$, independent of which YSZ was used. When the as-received NiO(A) or calcined NiO(C) was used, the final porosities were $70\% \pm 3\%$, in good agreement with the findings from a previous study.¹⁹

The lower porosity of samples prepared with NiO(B) were correlated with a higher shrinkage of the green tapes. Shrinkage with NiO(B) was found to be $\sim 35\%$, compared with a value of 25% with NiO(A) and Ni(C). The different shrinkage of the sample made with NiO(B) was probably related to the ratio of NiO and YSZ particle sizes, as has already been demonstrated in the literature.^{22,26}

The most interesting result from the use of NiO pore formers is shown in Fig. 8, which presents SEM micrographs of ceramic wafers prepared with YSZ(A) and either NiO(B), NiO(A), or NiO(C). All the samples have the appearance of a highly porous ceramic sponge with very uniform particle size distributions. However, the pore dimensions clearly change in a regular manner with the NiO particle size used in the preparation of the ceramic. Indeed, the characteristic pore dimensions correspond well with the initial particle size of the NiO given in Table I. Pores of 1–2 μm (Fig. 8(a)), 3–4 μm (Fig. 8(b)), and 10–15 μm (Fig. 8(c)) were observed using NiO particle sizes of 1, 4, and 16 μm , respectively. Therefore, the use of NiO as a pore former for the preparation of YSZ does allow control of the pore size distribution.¹⁹

Table IV. Porosity of YSZ Ceramics Produced from NiO–YSZ Composites

Sample	Porosity (vol%)
NiO(B)–YSZ(A)	$56\% \pm 1\%$
NiO(C)–YSZ(A)	$70\% \pm 1\%$
NiO(A)–YSZ(A)	$69\% \pm 1\%$
NiO(C)–YSZ(B)	$73\% \pm 1\%$
NiO(B)–YSZ(B)	$55\% \pm 1\%$

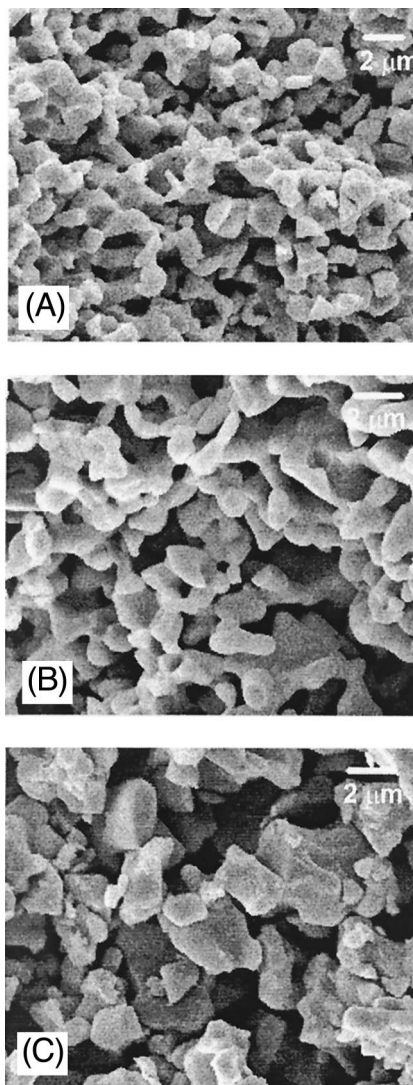


Fig. 8. SEM micrograph of porous YSZ produced from NiO–YSZ composites using YSZ(A) and (a) NiO(B), (b) NiO(A), and (c) NiO(C).

IV. Discussion

There is obviously much literature on the use of pore formers to achieve porous ceramics.¹ What we have tried to do here is to develop procedures specific to preparing highly porous high-temperature YSZ with controlled porosity and pore structure. This has been largely accomplished. The primary application for these materials is in the synthesis of copper-based anodes for SOFC; however, it is likely that these materials could find other applications as well.

Our results with pyrolyzable pore formers agreed well with the comprehensive investigations of Corbin and co-workers,⁹ who studied the effect of graphite loading and polymer content on tape shrinkage and final ceramic porosity for YSZ. As in their reports, we found that the total volume of pores depended on the loading of pore former. Also in both studies, the shape of the pores was related to the shape of the graphite pore former. As a result, we extended our study to include polyethylene and PMMA pore formers. Finally, in agreement with their results, shrinkage of the tapes did not depend on pore former loading.

It is interesting to consider the mechanisms behind pore formation. In the case of PMMA, the pore formers have been removed from the green tape by 700 K, while the main densification of the ceramic occurred above 1500 K, as indicated by both the shrinkage and loss of porosity of the tapes without pore formers. Clearly, pore structure had already been imprinted on the

ceramic at relatively low temperatures. The shape of the pores and the fact that porosity increased with the mass of the pore formers, independent of which pyrolyzable pore former (graphite, PMMA, or polyethylene) was used, indicated that the pore formers must act as templates. Corbin and co-workers⁹ made similar arguments but noted that templating alone could not result in interconnected pores unless the amount of pore former used reached the percolation threshold. At low pore former loadings, the pores should not be accessible to the external surface, while the measurements performed by both them and us showed accessible pores at very low loadings. Corbin and co-workers⁹ argued that additional pore volume must be introduced by oxide particle bridging, which was also necessary to explain our findings.

The use of NiO as a pore former appears to offer an additional level of control for determining the pore size distribution; however, the additional acid leaching step may make the use of NiO impractical for most applications. Still, it may be useful in some applications, possibly in conjunction with the use of pyrolyzable pore formers.²⁹ One interesting aspect of the NiO results is that they provide information on the structure of the initial Ni-YSZ cermets from which they are made. It has been demonstrated the particle sizes for NiO and YSZ affect the performance of Ni-cermet anodes in SOFCs, probably due to the resulting domain sizes for the nickel and YSZ phases.^{21,22} Porosity in the leached samples provides direct evidence for those changes in domain size and confirms the picture that has been proposed.

V. Conclusions

We have demonstrated that highly porous YSZ ceramics can be prepared through the use of either pyrolyzable pore formers or by acid leaching of nickel from Ni-YSZ cermets. The size and shape of pores produced by these pore formers are similar to those of the initial pore formers, so that good control of pore size and microstructure can be obtained in YSZ ceramics.

Acknowledgments

The authors thank Mr. Steve McIntosh for helping with the TPO studies and Ms. Yingyi Huang for help in sample preparation.

References

- ¹K. Ishizaki, S. Komarneni, and M. Nauko, "Porous Materials Process Technology and Applications," Kluwer, London, U.K., 1998.
- ²D. A. Hirschfeld, T. K. Li, and D. M. Liu, "Processing of Porous Oxide Ceramics," *Key Eng. Mater.*, **115**, 65–79 (1996).
- ³X. W. Zhu, D. L. Jiang, and S. H. Tan, "Impregnating Process of Reticulated Porous Ceramics Using Polymeric Sponges as the Templates," *J. Inorg. Mater.*, **16**, 1144–50 (2001).
- ⁴J. Luyten, J. Coymans, A. De Wilde, and I. Thijs, "Porous Materials: Synthesis and Characterization," *Key Eng. Mater.*, **206–213**, 1937–40 (2002).

- ⁵P. Colombo, "Ceramic Foams: Fabrication, Properties, and Applications," *Key Eng. Mater.*, **206–213**, 1913–18 (2002).
- ⁶O. Lyckfeldt and J. M. F. Ferreira, "Processing of Porous Ceramics by Starch Consolidation," *J. Eur. Ceram. Soc.*, **18**, 131–40 (1998).
- ⁷S. F. Corbin and P. S. Apte, "Engineered Porosity via Tape Casting, Lamination and the Percolation of Pyrolyzable Particulates," *J. Am. Ceram. Soc.*, **82** [7] 1693–701 (1999).
- ⁸T. Fukasawa, M. Ando, T. Ohji, and S. Kanzaki, "Synthesis of Porous Ceramics with Complex Pore Structure by Freeze-Dry Processing," *J. Am. Ceram. Soc.*, **84**, 230–32 (2001).
- ⁹S. F. Corbin, J. Lee, and X. Qiao, "Influence of Green Formulation and Pyrolyzable Particulates on the Porous Microstructure and Sintering Characteristics of Tape Cast Ceramics," *J. Am. Ceram. Soc.*, **84**, 41–47 (2001).
- ¹⁰S. Park, J. M. Vohs, and R. J. Gorte, "Tape Cast Solid Oxide Fuel Cells for the Direct Oxidation of Hydrocarbons," *J. Electrochem. Soc.*, **148**, A443–47 (2001).
- ¹¹E. Carlström and A. Kristoffersson, "Water Based Tape Casting and Manufacturing of Laminated Structure," *Key Eng. Mater.*, **206–213**, 205–10 (2002).
- ¹²J. B. Davis, A. Kristoffersson, E. Carlström, and W. J. Clegg, "Fabrication and Crack Deflection in Ceramic Laminates with Porous Interlayers," *J. Am. Ceram. Soc.*, **83**, 2369–74 (2000).
- ¹³S. Park, R. Craciun, J. M. Vohs, and R. J. Gorte, "Direct Oxidation of Hydrocarbons in a Solid Oxide Fuel Cell: I. Methane Oxidation," *J. Electrochem. Soc.*, **146** [10] 3603–605 (1999).
- ¹⁴S. Park, J. M. Vohs, and R. J. Gorte, "Direct Oxidation of Hydrocarbons in a Solid Oxide Fuel Cell," *Nature (London)*, **404**, 265–67 (2000).
- ¹⁵H. Kim, S. D. Park, J. M. Vohs, and R. J. Gorte, "Direct Oxidation of Liquid Fuels in a Solid Oxide Fuel Cell," *J. Electrochem. Soc.*, **148** [7] A693–95 (2001).
- ¹⁶R. J. Gorte, S. Park, J. M. Vohs, and C. Wang, "Anodes for Direct Oxidation of Dry Hydrocarbons in a Solid Oxide Fuel Cell," *Adv. Mater.*, **12**, 1465–69 (2000).
- ¹⁷R. Craciun, S. Park, R. J. Gorte, J. M. Vohs, C. Wang, and W. Worrell, "A Novel Method for Preparing Anode Cermets for Solid Oxide Fuel Cells," *J. Electrochem. Soc.*, **146**, 4019–22 (1999).
- ¹⁸D. W. Dees, T. D. Claar, T. E. Easler, D. C. Fee, and F. C. Mrazek, "Conductivity of Porous Ni/ZrO₂-Y₂O₃ Cermets," *J. Electrochem. Soc.*, **134**, 2141 (1987).
- ¹⁹H. Kim, C. daRosa, M. Boaro, J. M. Vohs, and R. J. Gorte, "Fabrication of Highly Porous YSZ by Acid Leaching Ni from a Ni-YSZ Cermet," *J. Am. Ceram. Soc.*, **85**, 1473–76 (2002).
- ²⁰N. Q. Minh, "Ceramic Fuel Cells," *J. Am. Ceram. Soc.*, **76** [3] 563–88 (1993).
- ²¹C.-H. Lee, C.-H. Lee, H.-Y. Lee, and S.-M. Oh, "Microstructure and Anodic Properties of Ni/YSZ Cermets in Solid Oxide Fuel Cells," *Solid State Ionics*, **98**, 39–48 (1997).
- ²²S.-P. Jiang, P. J. Callus, and S. P. S. Badwal, "Fabrication and Performance of Ni/3 mol% Y₂O₃-ZrO₂ Cermet Anodes for Solid Oxide Fuel Cells," *Solid State Ionics*, **132**, 1–14 (2000).
- ²³M. Brown, S. Primdahl, and M. Mogensen, "Structure/Performance Relations for Ni/Yttria-Stabilized Zirconia Anodes for Solid Oxide Fuel Cells," *J. Electrochem. Soc.*, **147**, 475–85 (2000).
- ²⁴J.-H. Lee, H. Moon, H.-W. Lee, J. Kim, J.-D. Kim, and K.-H. Yoon, "Quantitative Analysis of Microstructure and its Related Electrical Property of SOFC Anode, Ni-YSZ Cermet," *Solid State Ionics*, **148**, 15–26 (2002).
- ²⁵D.-M. Liu, "Influence of Dispersant on Powders Dispersion and Properties of Zirconia Green Compacts," *Ceram. Int.*, **26**, 279–87 (2000).
- ²⁶T. Matsushima, H. Ohri, and T. Hirai, "Effects of Sinterability of YSZ Powder and NiO Content on Characteristics of Ni-YSZ Cermets," *Solid State Ionics*, **111**, 315–21 (1998).
- ²⁷J. A. Lewis, "Binder Removal from Ceramics," *Ann. Rev. Mater. Sci.*, **27**, 147–73 (1997).
- ²⁸L. A. Salam, R. D. Matthews, and H. Robertson, "Pyrolysis of Poly-methyl Methacrylate (PMMA) Binder in Thermoelectric Green Tapes Made by the Tape Casting Method," *J. Eur. Ceram. Soc.*, **20**, 335–45 (2000).
- ²⁹T. Nishikawa, A. Takano, S. Furukawa, S. Honda, and H. Awaji, "Preparation and Properties of Porous Zirconia/Nickel Composites," *J. Jpn. Soc. Mater. Sci.*, **49**, 606–10 (2000). □